Optical sensor of salt concentration: uncertainty evaluation

T.H. Kauffmann, M.D. Fontana

Optical sensor of salt concentration : uncertainty evaluation

Thomas H. Kauffmann*, Marc D. Fontana

Laboratoire Matériaux Optiques Photonique et Systèmes (LMOPS - EA 4423) / Université Paul Verlaine de Metz and Supélec - 2 rue E. Belin 57070 Metz, FRANCE

Abstract

We report on the uncertainty upon the concentration of NaCl in an aqueous solution, as determined from the change in intensity of the OH band within a new Raman optical sensor. The various sources of errors are considered and the standard uncertainty is calculated. The accuracy of the sensor is discussed according to the application.

Keywords: Raman sensor, salted solution, error analysis, measurement uncertainty

1. Introduction

Raman spectroscopy is a well known optical technique generally used to study the vibrational properties of different media (solid, liquid or gas) in order to get some information on the structure and phase transformations of the sample [1, 2]. In addition, a Raman spectrum can indirectly provide several information about this sample. Thus, the composition of a mixture can be derived from the positions of the different peaks, the mechanical stress from the shift of a particular line, and the partial order or disorder of the structure from the FWHM (Full Width at Half Maximum) of some lines [1, 2].

The Raman spectroscopy is a contactless technique allowing, in situ and fast measurements (sometimes less than one second), so that it can be integrated in sensors to probe some physical properties of a substance [3, 4].

*Corresponding author

Email addresses: thomas.kauffmann@metz.supelec.fr (Thomas H. Kauffmann), fontana@metz.supelec.fr (Marc D. Fontana)

The spectroscopic instrument used as a sensor is often composed by many elements (laser source, optical components, spectrometer, camera...) which are all causes of measurement uncertainties. Moreover, the applied method and the signal processing used to extract the information of the signal are also sources of uncertainties.

We have recently conceived a new Raman sensor to detect the sodium chloride (NaCl) in an aqueous solution which is able to determine its concentration [3] or its phase [4, 5] (solid or liquid). The probe is based on the measurement of the integrated intensity of the Raman stretching OH band in salted solutions. The ratio between two parts of the spectrum gives a parameter, S_D, which provides the concentration at a given temperature from an appropriate calibration [4]. The main application devoted to this sensor is the control of the use of NaCl as de-icer by the road winter service, so that these last investigations had specially covered the large concentrations (above 50 g/l). The sensor could be interesting as well to detect low concentrations of NaCl in basins or rivers.

Here, the various sources of the measurement uncertainties in the case of wide (0 up to 200 g/l) and low (0 up to 15 g/l) concentration range are evaluated and discussed.

2. Sensor description and method

2.1. NaCl concentration determination

Our experimental method is based on the detection by Raman spectroscopy of the OH-stretching band of water [6]. This broad band lying between 2800 and 3860 cm^{-1} was shown to be affected by the NaCl incorporation in the water [7]. This change is reflected by an increase of the intensity of the upper part of the band and a simultaneous decrease of the lower part, as shown in Figure 1.

As a consequence, our method to determine the concentration of the NaCl consists into the calculation of the ratio between the integrated intensity of these two areas, J_1 and J_2, which are affected by the concentration. This parameter S_D parameter is therefore defined by:

$$S_D = \frac{J_1}{J_2} = \frac{\int_{3330}^{3860} I(w) \cdot dw}{\int_{2800}^{3330} I(w) \cdot dw} \quad (1)$$

where w is the wavenumber and I the intensity. The main advantages of this method considering the ratio of integrated intensities are to avoid the

deconvolution of the spectrum, to discard the effect of the spectrometer drift and to reduce the influence of the measurement noise.

The signal treatment is trivial and consists in recording directly the Raman spectrum from the CCD camera and in applying several treatments on the useful area (OH-stretching band): baseline correction, intensities normalization and smoothing. Then the two areas, J_1 and J_2, are calculated in order to get the S_D ratio. The last part of the treatment consists in using a calibration $S_D = f(C)$ to determine the concentration value C.

2.2. Instrumentation and calibration

The main part of our optical sensor (see Figure 2) is composed by a Raman spectrometer including a laser diode (*Laser Quantum Ventus*) with an exciting line at the wavelength of 532 nm and an output power of 300 mW, an optical head with a Notch filter and a Si CCD camera (*Andor technology*) of 1024x256 pixels (26 μm^2) cooled at -70 °C. The Raman spectrometer (*Horiba scientific HE*) has a grating of 920 g/mm and a spectral range from 975 to 3870 cm^{-1} with a spectral resolution of 3 cm^{-1}. The CCD is linked to the computer by an USB plug and the two optical fibers for the excitation and for the collection have a core diameter of 100 μm. The laser light is focused on the sample through a 50X longworking-distance objective (*Olympus*) at about 8 mm.

The calibration of the sensor was obtained from the study of the dependence of the parameter S_D on the solution concentrations which was determined by the titration method with silver nitrate $AgNO_3$.

To achieve the calibration of our probe several measurements were done on NaCl solutions with different concentrations at various temperatures. Indeed the Raman OH-stretching band of the water spectrum is not only affected by the NaCl concentration but also by the temperature, as shown in Figure 3. Two different calibrations of the sensor were done according to the aimed applications. The first calibration concerns the wide concentration range from 0 to 200 g/l with a step of 10 g/l with a temperature excursion from 0 to 10 °C with a step of 0.5 °C. A temperature stage (*Linkam THMS600*) controlled by computer was used to realize this excursion. The second series of measurements were carried out for low NaCl concentrations from 0 to 15 g/l with a step of 1 g/l, from 0 to 30 °C with a step of 0.5 °C.

Each value of S_D was obtained from the measurement of the Raman integrated intensities on a salted solution, within constant experimental conditions and the same integrated time (10 accumulations of 1 second in order

to reduce the random spectral noise). 21 samples of salted solutions with varying concentration from 0 to 200 g/l were used to get the calibration for the wide range and 16 samples from 0 to 15 g/l were used to achieve the calibration for the low concentration range.

In Figures 4a and 4b are plotted the calibrations recorded for different temperatures for the wide and low range of concentration respectively. According to a linear fit applying the least square method, the calibration equation can be expressed for each range by $\hat{S}_D = a \cdot C + b$ where $\hat{S}_D$ is the predicted value of S_D, a is the slope and b the y-intercept. It is observed in Table 1 that the slope a between $\hat{S}_D$ and the concentration C is nearly independent of the temperature within each concentration range. By contrast, b strongly varies with the temperature in both concentration ranges.

3. Measurement uncertainty calculation

At first it is reminded that according to the ISO GUM [8], the standard measurement uncertainty can be evaluated via two kinds of methods. The type A evaluation consists into a statistical study from several measurements of the same quantity obtained in assumed constant experimental conditions. The result is chosen as the average of the data and the standard uncertainty is given by the standard deviation of the mean. Uncertainty evaluation by means other than statistical analysis provides the type B contributions.

In our case of the probe of NaCl concentration the different sources of uncertainty are as follows. The calibration gives to rise to a origin of uncertainty linked to the linear regression which is evaluated by a type A method. Then the error in the titration of the sample solution and the error on the measurement of the integrated intensities have to be taken into account. The effect on the determination of the concentration is thus calculated for each source of error. Finally the influence of the temperature on the accuracy of our sensor is considered and evaluated.

In the calculation of the whole uncertainty on the concentration, the squared of standard uncertainties obtained on the various sources of error have to be added. To deduce the standard uncertainty from the experimental uncertainty of type B, a rectangular distribution is conventionally assumed since no indication of the confidence, with which the error was estimated, was supplied by the constructor of the different used instruments.

3.1. Uncertainty related to the calibration

The confidence on the calibration depends on the reliability of the results derived from the fit of the plot $S_D = f(C)$ with a regression linear law $\hat{S}_{Di} = a \cdot C_i + b$. For this we apply the type A method and calculate the standard deviation between experimental data of S_D and the values as predicted by the law [9, 10]:

$$s(S_D) = \frac{1}{\sqrt{n-2}} \cdot \sqrt{\sum_{i=1}^{n} (S_{Di} - \hat{S}_{Di})^2} \tag{2}$$

where S_{Di} and $\hat{S}_{Di}$ are the experimental and predicted values respectively and n is the number of data used for the calibration. Then we calculate the standard uncertainty on the concentration C coming from the linear regression by the inverse calibration method with the formula [10, 11]:

$$u_{calib}(C) = \frac{s(S_D)}{a} \cdot \sqrt{\frac{1}{N} + \frac{1}{n} + \frac{(S_D - \overline{S_D})^2}{a^2 \cdot \sum_{i=1}^{n} (C_i - \overline{C})^2}} \tag{3}$$

where $s(S_D)$ is given by equation (2), S_D is the value coming from N replicates, $\overline{S_D}$ and $\overline{C}$ are the averages of the calibration values and C_i the different concentration values used in the calibration.

3.2. Uncertainty on the titration

The titration of the NaCl solutions used as samples in the calibration procedure is determined with an uncertainty of $\Delta C = \pm 0.1$ g/l. By applying a rectangular distribution for this type B evaluation, the concentration uncertainty related to the titration is given by $u_{titr}(C) = \Delta C/\sqrt{3}$.

3.3. Instrumental uncertainty

There are concerned the uncertainties $u_{instr}(S_D)$ related to the measurement of the S_D ratio which depends on the characteristics of the instruments (spectrometer, laser power, ...). The S_D ratio is rewritten from equation (1) as:

$$S_D = \frac{J_2}{J_1} = \frac{I_2 \cdot dw_2}{I_1 \cdot dw_1} \tag{4}$$

where I_1 and I_2 are the intensity average of the two areas, respectively J_1 and J_2, and dw_1 and dw_2 the two Raman ranges used for the areas calculation.

We can therefore deduce the relative standard uncertainty of the S_D ratio by:

$$(\frac{u(S_D)}{S_D})^2 = (\frac{u(I_2)}{I_2})^2 + (\frac{u(dw_2)}{dw_2})^2 + (\frac{u(I_1)}{I_1})^2 + (\frac{u(dw_1)}{dw_1})^2 \quad (5)$$

where $u(I)$ and $u(dw)$ are respectively the standard uncertainty on the intensity I and the wavenumber range dw. The two chosen areas have the same width so that $dw_1 = dw_2 = dw$ and assuming that we have $I_1 \approx I_2 \approx I$, it comes:

$$(\frac{u(S_D)}{S_D})^2 = 2 \cdot (\frac{u(I)}{I})^2 + 2 \cdot (\frac{u(dw)}{dw})^2 \quad (6)$$

The uncertainty of the intensity I, which is in fact the spectral noise, is estimated at $\pm 0.5\%$ of the spectrum intensity in the optimal condition measurement and the uncertainty of the Raman shift is given by the constructor and is equal to $\pm 1/2$ pixel. This value represents for our spectrometer an uncertainty of ± 1.5 cm^{-1} for a band half width of 530 cm^{-1}, i.e. a relative uncertainty of $\pm 0.3\%$. The standard uncertainties $u(I)$ of the intensity and $u(dw)$ of the Raman shift are estimated with a rectangular distribution for a type B evaluation.

It is to be mentioned that the drift of the spectrometer causing a shift of the Raman peaks positions is here assumed to be negligible with respect to other errors entering. In fact to diminish this drift a calibration of spectrometer by means of the position peak of Si was made between each series of measurements.

Finally we can find the standard concentration uncertainty related to the instruments by dividing the uncertainty on S_D by the slope a of the calibration:

$$u_{instr}(C) = \frac{S_D \cdot \sqrt{2}}{a} \cdot \sqrt{(\frac{0.005}{\sqrt{3}})^2 + (\frac{0.003}{\sqrt{3}})^2} \quad (7)$$

3.4. Whole standard uncertainty

The combined standard uncertainty of the concentration can be now obtained by adding the squared values of each uncertainty coming from different error sources, i.e. from the calibration (type A evaluation) and from the titration and the instrumentation (type B evaluations):

$$u_c(C) = \sqrt{u^2_{calib}(C) + u^2_{titr}(C) + u^2_{instr}(C)} \quad (8)$$

4. Temperature influence

We have observed above a strong influence of the temperature on the Raman spectrum of the OH-stretching band so that the defined parameter S_D is affected by the NaCl solution temperature as well (see Figures 4a and 4b). The temperature therefore can play the role, as frequently in sensors, of an influence external parameter which can impede a correct determination of the quantity to be found. The temperature T is therefore an additional source of error for the concentration determination. For this we establish the relationship between a temperature variation and the measured parameter S_D, in our probe when the concentration is assumed to be constant. This leads to perform an additional calibration S_D vs T.

4.1. Calibration $S_D = f(T)$

In Figure 5 is plotted the $S_D = f(T)$ for three different NaCl concentrations. It is pointed out that even a relatively small temperature change can give rise to a large variation of the parameter S_D, used in the determination of the NaCl content with our sensor. Thus a variation of T of about 5 °C causes nearly the same shift of S_D as a change of concentration of 10 g/l. This has as first consequence that S_D has to be recorded considering both the salt concentration and the temperature. The second effect concerns the additional error on the predicted value of S_D, and to the salt content.

The temperature dependences reported in Figure 5 are linear, for each concentration so that $\hat{S}'_D = a' \cdot T + b'$ where $\hat{S}'_D$ is the predicted value of S_D, a' is the slope and b' the y-intercept. The linear regression of these plots was obtained by applying the least square method. We calculate the standard deviation $s'(S_D)$ between measured and predicted values of S_D for p different temperatures by:

$$s'(S_D) = \frac{1}{\sqrt{p-2}} \cdot \sqrt{\sum_{i=1}^{p} (S_{Di} - \hat{S}'_{Di})^2} \tag{9}$$

Thus we can obtain the standard uncertainty $u_{Tcalib}(S_D)$ of the S_D ratio due to the temperature calibration by applying the formula:

$$u_{Tcalib}(S_D) = s'(S_D) \cdot \sqrt{\frac{1}{N'} + \frac{1}{p} + \frac{(S_D - \overline{S_D})^2}{a'^2 \cdot \sum_{i=1}^{p} (T_i - \overline{T})^2}} \tag{10}$$

where $s'(S_D)$ is given by equation (9), S_D is the value coming from N' replicates, $\overline{S_D}$ and $\overline{T}$ are the averages of the temperature calibration values and T_i the different temperature values used in the calibration.

4.2. Temperature stage uncertainty

Then the uncertainty of the temperature T is given by the temperature stage constructor as equal to $\Delta T = \pm 0.1$ °C. We apply therefore a type B evaluation with a rectangular distribution to find $u(T) = \Delta T/\sqrt{3}$. In order to determine the uncertainty on S_D caused by the error on the temperature, the standard temperature uncertainty is then multiplied by the slope a' of the temperature calibration $u_{Tstage}(S_D) = a' \cdot u(T)$.

4.3. Concentration uncertainty due to the temperature influence $u_T(C)$

The standard uncertainty on the concentration due to the temperature influence can be evaluated by associating the two above uncertainties of the S_D ratio and by dividing the value by the slope a of the concentration calibration:

$$u_T(C) = \sqrt{\frac{u^2_{Tcalib}(S_D) + u^2_{Tstage}(S_D)}{a^2}} \tag{11}$$

4.4. Whole concentration uncertainty

At last we combine the uncertainty due to the temperature influence to the uncertainty calculated above arising from the intrinsic sources of errors of type A and B associated to the proposed method:

$$u_{c,T}(C) = \sqrt{u^2_c(C) + u^2_T(C)} \tag{12}$$

Finally the expanded uncertainty $U_{c,T}(C)$ of the concentration for a confidence level of 95% is given by $U_{c,T}(C) = k \cdot u_{c,T}(C)$ with a coverage factor of $k = 2$.

5. Numerical applications and discussion

5.1. Results for the wide range of concentration

Calculations in wide range of concentration (0-200 g/l) are illustrated for a concentration of 50 g/l at a temperature of 10 °C. At this working point S_D is equal to 1.3511 and the calibration equations are $S_D = 0.004380 \cdot C + 1.1412$ for the concentration and $S_D = 0.009205 \cdot T + 1.2666$ for the temperature.

We calculate first the concentration uncertainty regardless the temperature influence. We get a standard deviation between experimental and predicted data in the concentration calibration equal to $s(S_D) = 1.1 \cdot 10^{-2}$ and with $N = 10$ replicates, $n = 21$ samples, $\overline{S_D} = 1.5792$ and $\overline{C} = 100$ g/l we find an uncertainty $u_{calib}(C) = 1.1$ g/l. Then with a titration uncertainty for the NaCl solutions of $\Delta C = 0.1$ g/l we find $u_{titr}(C) = 0.1/\sqrt{3} = 0.06$ g/l. The standard uncertainty related to the instruments is found to be $u_{instr}(S_D) = 6.4 \cdot 10^{-3}$ so that we get $u_{instr}(C) = 1.5$ g/l. Finally the combined standard uncertainty of the concentration is found equal to $u_c(C) = \sqrt{1.1^2 + 0.06^2 + 1.5^2} = 1.9$ g/l and with a coverage factor of $k = 2$ we find an expanded uncertainty of $U_c(C) = 3.8$ g/l.

Then we evaluate the concentration uncertainty due to the temperature influence. We find $s'(S_D) = 3.6 \cdot 10^{-3}$ as standard deviation between experimental and predicted data. Then with $N' = 10$ replicates, $\overline{S_D} = 1.3126$ and $\overline{T} = 5$ °C we obtain $u_{Tcalib}(S_D) = 1.4 \cdot 10^{-3}$. From the uncertainty on the temperature stage given by the constructor (±0.1 °C) we get $u(T) = 0.1/\sqrt{3} = 0.06$ °C and then by multiplying by the slope a' we obtain $u_{Tstage}(S_D) = 5.5 \cdot 10^{-4}$. Finally we calculate the standard uncertainty on the concentration due to the temperature by associating the two above uncertainties and by dividing the value by the slope a of the concentration calibration:

$$u_T(C) = \sqrt{\frac{(1.4 \cdot 10^{-3})^2 + (5.5 \cdot 10^{-4})^2}{0.004380^2}} = 0.3 g/l. \tag{13}$$

At last we combine the uncertainty due to the temperature influence with the uncertainty coming from the other sources (calibration, titration, instruments) to get the total concentration uncertainty $u_{c,T}(C) = \sqrt{1.9^2 + 0.3^2} = 1.9$ g/l. Finally the expanded uncertainty of the concentration with a confidence level of 95% is $U_{c,T}(C) = 2 * 1.9 = 3.8$ g/l for $C = 50$ g/l and $T = 10$ °C.

5.2. Results for the low range of concentration

To illustrate the case of the low range of concentration (0-15 g/l), calculations of the uncertainty are given for a concentration of 10 g/l at a temperature of 20 °C. At this working point S_D is equal to 1.3042 and the calibration equations are $S_D = 0.003602 \cdot C + 1.2682$ for the concentration and $S_D = 0.008402 \cdot T + 1.1401$ for the temperature.

We proceed with the same way as for the wide concentration range. Thus we find a standard deviation between experimental and predicted data coming from the procedure equal to $s(S_D) = 2.3 \cdot 10^{-3}$ and with $N = 10$ replicates, $n = 16$ samples, $\overline{S_D} = 1.2952$ and $\overline{C} = 7.5$ g/l we get an uncertainty $u_{calib}(C) = 0.3$ g/l. The titration uncertainty is unchanged and equal to $u_{titr}(C) = 0.06$ g/l. The standard uncertainty related to the instruments is $u_{instr}(S_D) = 6.2 \cdot 10^{-3}$ giving rise to $u_{instr}(C) = 1.7$ g/l. Finally the combined standard uncertainty of the concentration is found equal to $u_c(C) = \sqrt{0.3^2 + 0.06^2 + 1.7^2} = 1.7$ g/l and with a coverage factor of $k = 2$ we find an expanded uncertainty of $U_c(C) = 3.4$ g/l.

The temperature calibration was made for the low range between 0 °C and 30 °C by a step of 0.5 °C i.e. $p = 61$ samples. We find $s(S_D) = 5.4 \cdot 10^{-3}$ as standard deviation between experimental and predicted data within the temperature calibration and with $N' = 10$ replicates, $\overline{S_D} = 1.2661$ and $\overline{T} = 15$ °C we obtain $u_{Tcalib}(S_D) = 1.9 \cdot 10^{-3}$. Then with the temperature stage uncertainty given by the constructor we find $u_{Tstage}(S_D) = 0.008402 * 0.06 = 5 \cdot 10^{-4}$. Finally we calculate the standard uncertainty on the concentration due to the temperature by:

$$u_T(C) = \sqrt{\frac{(1.9 \cdot 10^{-3})^2 + (5 \cdot 10^{-4})^2}{0.003602^2}} = 0.5 g/l. \tag{14}$$

We note that the contribution related to the temperature stage uncertainty is negligible ($u_{Tstage}(C) = 0.1$ g/l) compared to the contribution coming from the calibration ($u_{Tcalib}(C) = 0.5$ g/l).

At last after associating the various sources of uncertainty we get the total concentration uncertainty $u_{c,T}(C) = \sqrt{1.7^2 + 0.5^2} = 1.8$ g/l and $U_{c,T}(C) = 3.6$ g/l for the low concentration 10 g/l at 20 °C.

5.3. Discussion

All the identified sources of uncertainty on the concentration as well as their relative contribution are summarized in Table 2 for the wide and low concentration ranges. They are defined by the ratio of the squared of considered standard uncertainties.

At first we note that the expanded uncertainty has nearly the same value for both concentration ranges. This gives rise to a good relative accuracy ($U/C < 10\%$) when probing large NaCl concentration (50 g/l) but a poor accuracy if our sensor is devoted to measure low concentration ($U/C \sim 25\%$ if $C = 15$ g/l).

If we look at the intrinsic origins of the uncertainty, it can be pointed out from Table 2 that the instrumental error has nearly the same value and provides the largest contribution for both concentration ranges. On the contrary, the uncertainty coming from the calibration procedure is large in the wide concentration range but negligible for low concentration measurements. This discrepancy arises from the much higher density of data (number of data within the concentration range) used in the last case.

The second remark concerns the temperature as an external parameter influencing the measurement and the sensor accuracy. Table 2 shows that the whole uncertainty has the same or nearly the same value if regarding or not the temperature effect for both concentration ranges. This observation does not mean that the temperature does not play an important role in the collecting data procedure with our sensor. In fact the reliability of the measurements depends on the knowledge of the calibration at the correct temperature. In other terms the non-accounting of the temperature should lead from the measured value of S_D to an erroneous determination of the concentration.

Our estimation of the different sources of errors to be considered within the sensor proposed to determine the salt concentration, provides a too large uncertainty if probing small values of concentration (36% for a concentration of 10 g/l). By contrast, the results should be more reliable if measuring concentration values larger than 50 g/l. In this case the relative accuracy should be reduced to 10% or less (3.8% for a concentration of 100 g/l). This better accuracy comes from the fact that the main error contribution is independent of the concentration values. This renders our optical sensor more efficient for applications for which large values of concentration are purchased [12]. In fact even for low concentrations, the accuracy of our sensor can be improved, regarding and analyzing results reported in Table 2.

The only source, on which we can efficiently act to reduce the total uncertainty of our sensor, is related to the instruments (spectrometer and detector). It is indeed possible to reduce the spectral noise by increasing the number of accumulations and collecting a larger signal in using a more powerful laser and increasing the exposure time.

Additionally CCD detector used in the calibration can be replaced by another one with more pixels (2048 instead of 1024 for example). In this case the resolution will be twice better with the same spectrometer grating (± 0.75 cm^{-1} for the same band width of 530 cm^{-1}) and the uncertainty due to the instruments can be recalculated to find $u_{instr}(C) = 1.5$ g/l instead of

1.7 g/l and a total concentration uncertainty $u_{c,T}(C) = 1.6$ g/l instead of 1.8 g/l for the low concentration range.

The useful Raman signal covers a spectral range of about 1060 cm^{-1} from 2800 cm^{-1} to 3860 cm^{-1} while the full spectral range with the current grating starts at 975 cm^{-1}. So a huge part of the range is useless in our method and the grating can therefore be replaced by another one with more grooves per millimeter in order to use all the CCD dimension and thus improve the spectral resolution.

6. Conclusion

In this study, was reported and discussed an estimation of uncertainty to be considered in a new Raman sensor to probe the NaCl concentration in a salted solution. This method provides quick, in situ and remote measurements. The various sources of uncertainties were taken into account and calculated. In particular, the influence of the temperature change during probing was pointed out and discussed. Based on the analysis of estimation of expanded uncertainty at 95% confidence level with a coverage factor of $k = 2$, the values of concentration measurement uncertainty were evaluated at 3.8 g/l for the wide range of concentration (0-200 g/l) and at 3.6 g/l for the low range (0-15 g/l). The concentration uncertainty is therefore nearly the same for the two ranges so that the sensor is better suitable for the high concentration applications.

The main application of this sensor is the road winter service with the measurement of high concentrations but other applications using small concentrations could be exploited by our sensor. In these cases a better accuracy is required and can be provided by a more appropriate choice and performances of instruments.

References

[1] Colomban, Ph., *Raman imaging of materials and heterogeneous devices*, Techniques de l'ingénieur, 2002, RE-5:13.

[2] L. Andrew Lyon, Christine D. Keating, Audrey P. Fox, Bonnie E. Baker, Lin He, Sheila R. Nicewarner, Shawn P. Mulvaney, and Michael J. Natan, *Raman spectroscopy*, Anal. Chem., 1998, 70, 341R-361R.

[3] Durickovic I., Claverie R., Marchetti M., Bourson P., Chassot J-M., Fontana M.D., *Experimental study of NaCl aqueous solutions by Raman spectroscopy : Towards a new optical sensor*, Applied Spectroscopy, 2010, 64, 853-857.

[4] Claverie R., Fontana M.D., Durickovic I., Bourson P., Marchetti M., Chassot J-M., *Optical Sensor for Characterizing the Phase Transition in Salted Solutions*, Sensors, 2010, 10, 3815-3823.

[5] Durickovic I., Claverie R., Bourson P., Marchetti M., Chassot J-M., Fontana M., *Water-ice phase transition probed by Raman spectroscopy*, Journal of Raman Spectroscopy, 2011, DOI: 10.1002/jrs.2841.

[6] Carey D., Korenowski G.,*Measurement of the Raman spectrum of liquid water*, Journal of Chemical Physics, 1998, vol. 108, n7, pp. 2669-2675.

[7] Terpstra P., Combes D., Zwick A.,*Effects of salts on dynamics of water: A Raman spectroscopy study*, Journal of Chemical Physics, 1990, vol. 92, pp. 65-70.

[8] *Guide to the Expression of Uncertainty in Measurement*, ISO, Geneva, 1995, ISBN 92-67-10188-9.

[9] Rosengard A., *Probabilités et statistiques en recherche scientifique*, Dunod, 1972, p178-194.

[10] Feinberg M., *Validation interne des méthodes d'analyse*, Techniques de l'ingénieur, 2001, P224-8.

[11] Lu T., Chen C., *Uncertainty evaluation of humidity sensors calibrated by saturated salt solutions*, Measurement 40, 2007, 591-599.

[12] Marchetti M., Claverie R., Durickovic I., Bourson P., Chassot J.-M., Fontana M., Livet J., Kauffmann T., *Détermination de la quantité résiduelle de fondants routiers par une technique spectroscopique sans contact*, Congrès AIPCR 2010, Québec (Canada).

Biographies

Marc D. Fontana was born in France in 1953. He received the PhD degree in physics in 1979 from the University Louis Pasteur, Strasbourg. His thesis was on the lattice dynamics and phase transitions in KNbO3. He became Assistant Professor at the University of Metz. Then, after a post-doctoral position at IBM Laboratories, Ruschlikon, Switzerland, and the Habilitation, he received the title of Professor at the University in 1988 and his interest turned to linear and non linear optics. He was head of the Laboratoire Matériaux Optiques Photonique et Systèmes (LMOPS) - University of Metz, from 1992 until 2008. He is the author of more than 150 papers.

Thomas H. Kauffmann was born in France in 1985. He received his engineer diploma (Dipl.-Ing.) in electronics from the National school of engineering ENSICaen of Caen in 2008. He specialized during his studies in optics, sensors and optoelectronics. After an internship, he joined the Laboratoire Matériaux Optiques, Photonique et Systèmes (LMOPS) in september 2008 as a research engineer in the team "control and optical sensors". His first project funded by the National Agency of Research of France (ANR) was to develop an optical sensor in order to determine and to optimize the salt concentration applied on roads in winter (de-icers).

Legends

Figure 1. Evolution of the Raman OH-stretching band with the NaCl concentration. In the insert is reported the whole OH band spectrum.
Figure 2. Experimental setup description.
Figure 3. Influence of the temperature on the Raman OH-stretching band of a NaCl solution at 10 g/l.
Figure 4a. Concentration calibration lines from 0 to 200 g/l (wide range) at different temperatures.
Figure 4b. Concentration calibration lines from 0 to 15 g/l (low range) at different temperatures.
Figure 5. Temperature dependence of the parameter S_D for different concentrations.
Table 1. Slope and intercept of the calibration linear fit for several temperatures and for the two concentration ranges.
Table 2. Uncertainties calculated for 50 g/l at 10 °C (wide concentration

range) and for 10 g/l at 20 °C (low concentration range).

Table 1

Wide concentration range		
Temperature	**Slope a**	**Intercept b**
5°C	0.004259	1.1087
10°C	0.004380	1.1412
Low concentration range		
Temperature	**Slope a**	**Intercept b**
15°C	0.003521	1.2273
20°C	0.003602	1.2682
25°C	0.003535	1.3154

Table 2

	Wide concentration range	
Source of uncertainty	**Standard uncertainty**	**Contribution**
Calibration $u_{calib}(C)$	1.1 g/l	$\sim 34\%$
Titration $u_{titr}(C)$	0.06 g/l	$< 1\%$
Instruments $u_{instr}(C)$	1.5 g/l	$\sim 62\%$
Temperature $u_T(C)$	0.3 g/l	$\sim 3\%$
Without temperature influence		
Combined standard uncertainty $u_c(C)$	1.9 g/l	
Expanded uncertainty $U_c(C)$ (k=2)	3.8 g/l	
With temperature influence		
Combined standard uncertainty $u_{c,T}(C)$	1.9 g/l	100%
Expanded uncertainty $U_{c,T}(C)$ (k=2)	3.8 g/l	
	Low concentration range	
Source of uncertainty	**Standard uncertainty**	**Contribution**
Calibration $u_{calib}(C)$	0.3 g/l	$\sim 3\%$
Titration $u_{titr}(C)$	0.06 g/l	$< 1\%$
Instruments $u_{instr}(C)$	1.7 g/l	$\sim 89\%$
Temperature $u_T(C)$	0.5 g/l	$\sim 8\%$
Without temperature influence		
Combined standard uncertainty $u_c(C)$	1.7 g/l	
Expanded uncertainty $U_c(C)$ (k=2)	3.4 g/l	
With temperature influence		
Combined standard uncertainty $u_{c,T}(C)$	1.8 g/l	100%
Expanded uncertainty $U_{c,T}(C)$ (k=2)	3.6 g/l	

Figure1

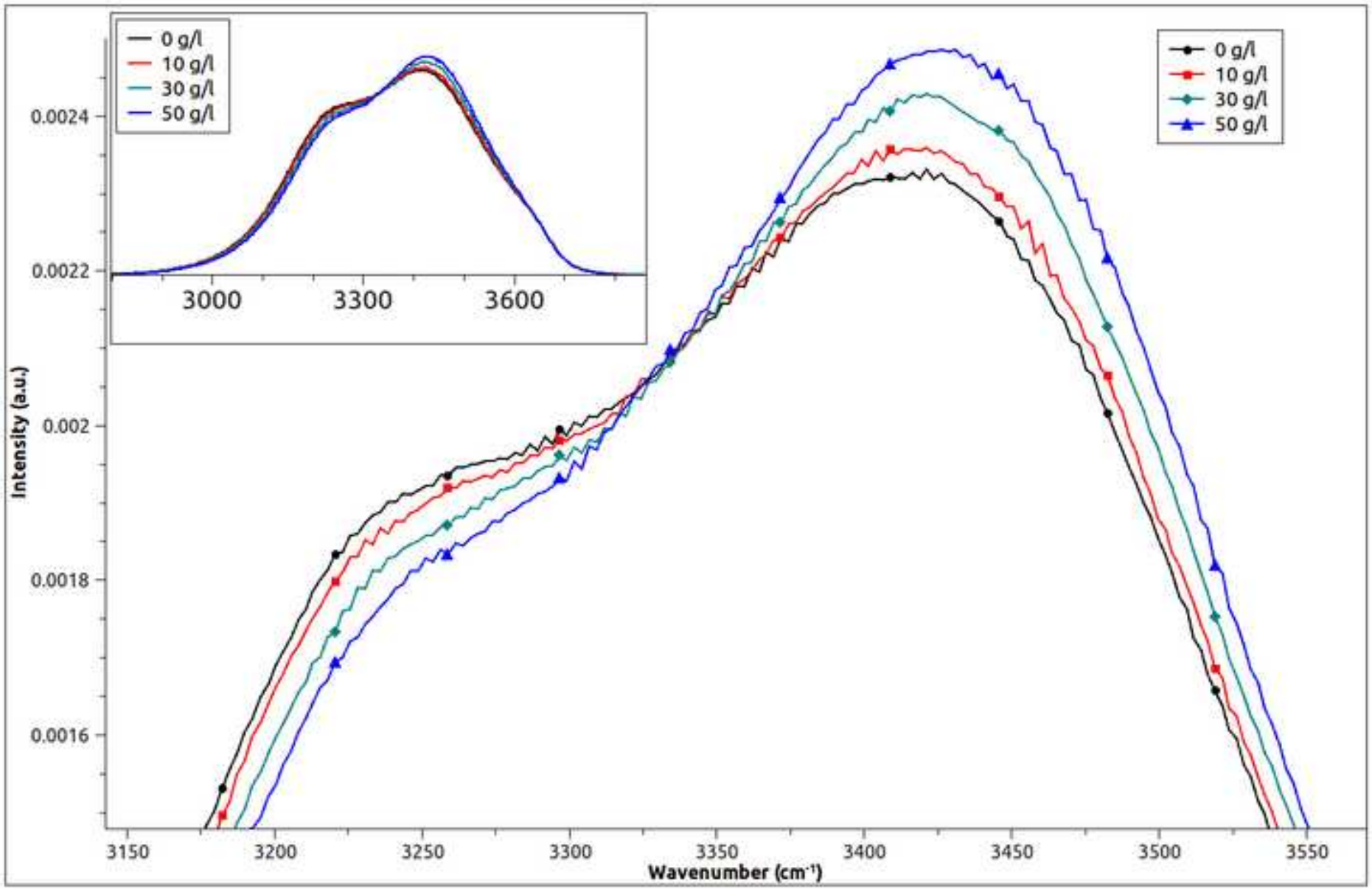
0 g/l
10 g/l
30 g/l
50 g/l
0.0024
0.0022
0.002
0.0018
0.0016
3000
3300
3600
Intensity (a.u.)
3150
3200
3250
3300
3350
3400
3450
3500
3550
Wavenumber (cm-1)

Figure2

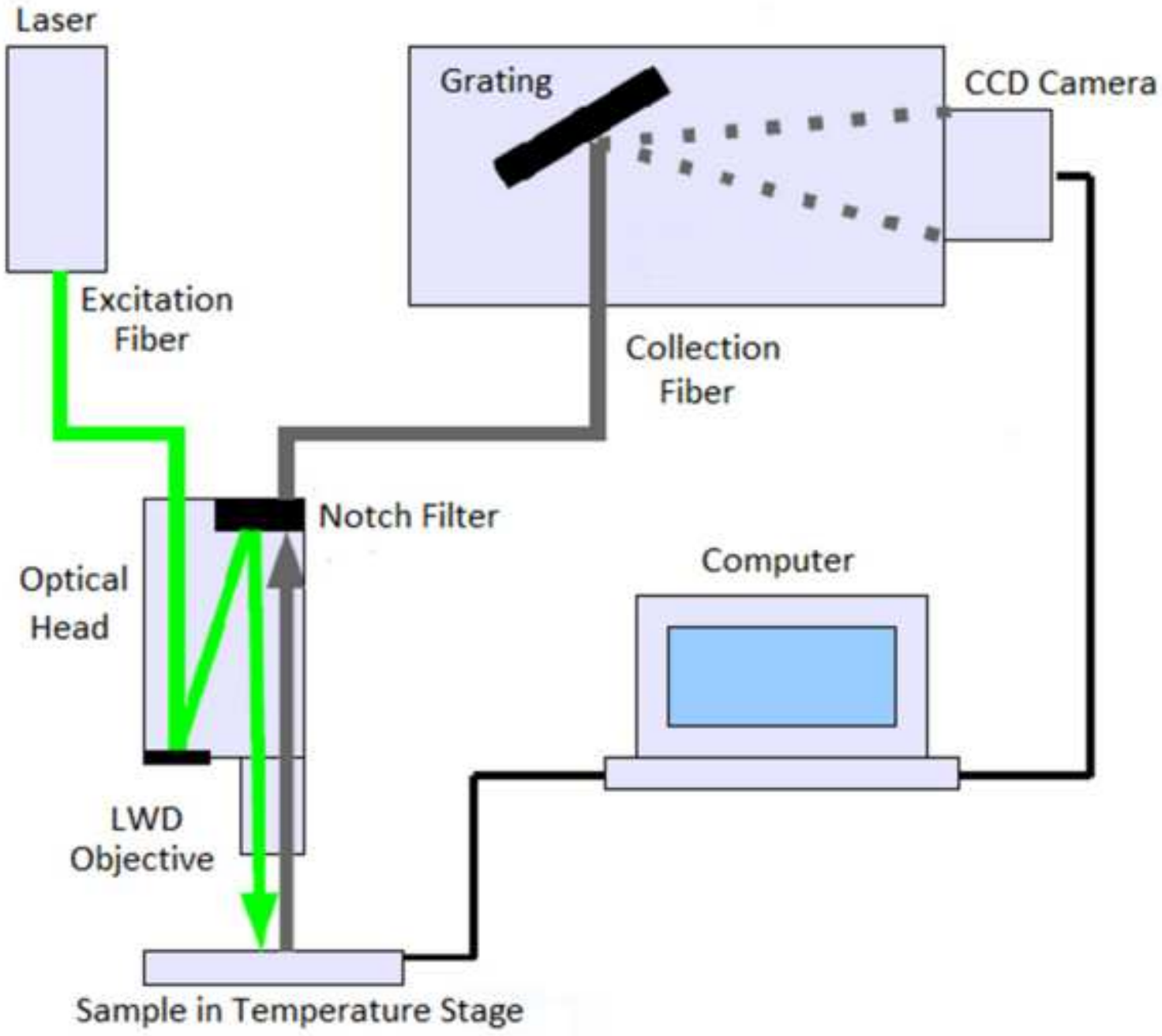
Laser
Grating
CCD Camera
Excitation Fiber
Collection Fiber
Notch Filter
Optical Head
Computer
LWD Objective
Sample in Temperature Stage

Figure3

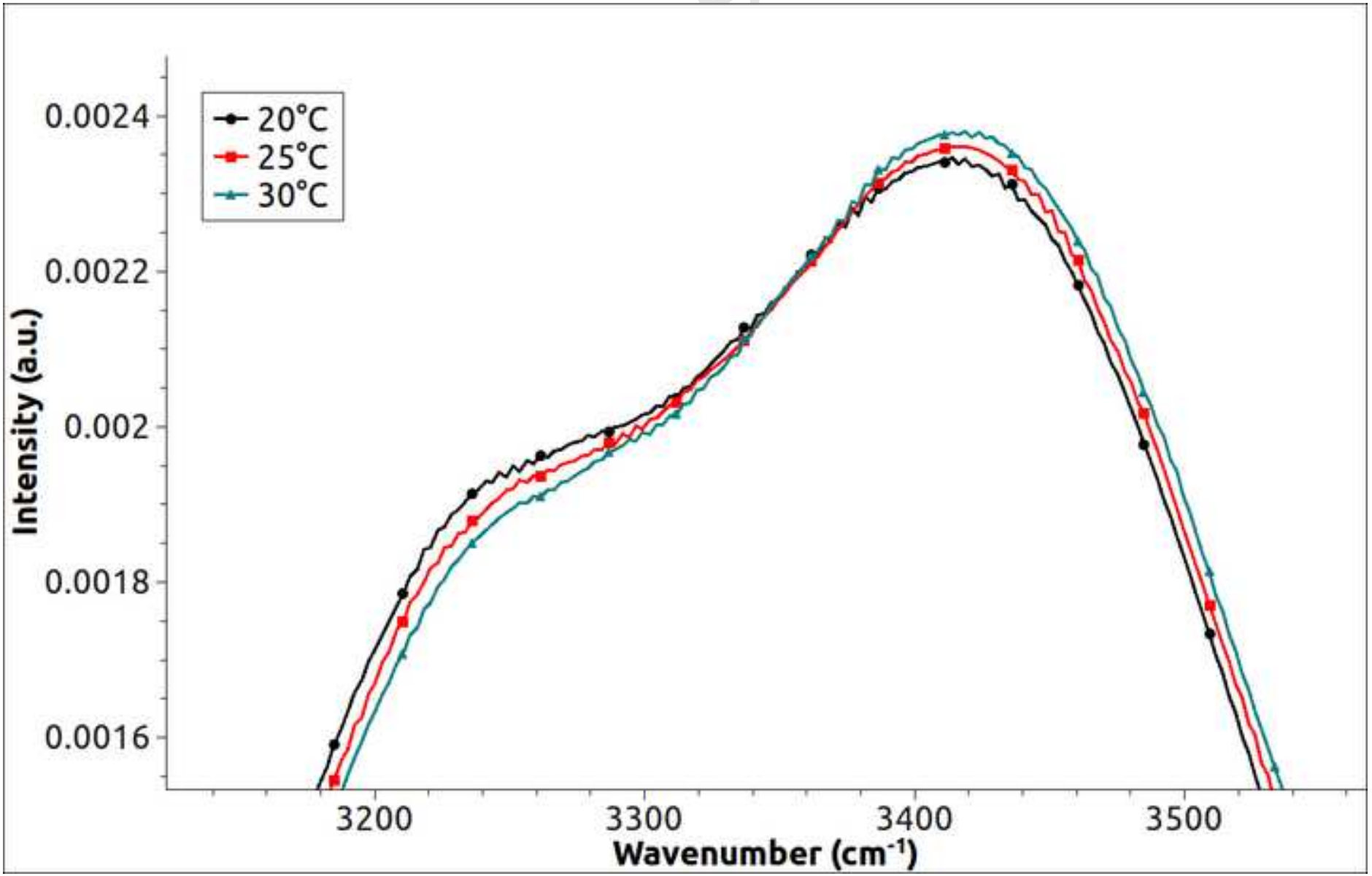
20°C
25°C
30°C
0.0024
0.0022
0.002
0.0018
0.0016
Intensity (a.u.)
3200
3300
3400
3500
Wavenumber (cm-1)

Figure4a

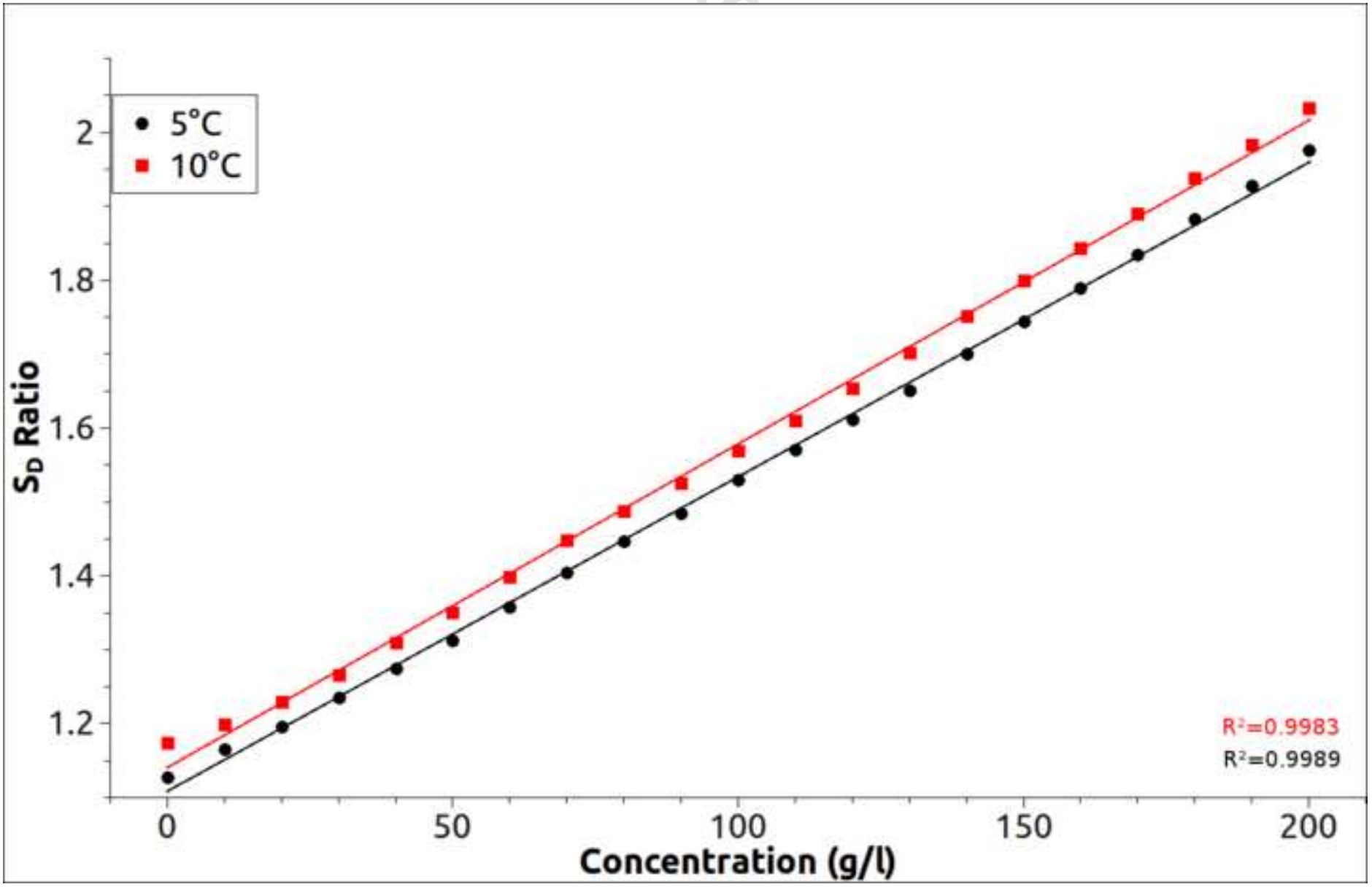
5°C
10°C
2
1.8
1.6
1.4
1.2
S_D Ratio
0
50
100
150
200
Concentration (g/l)
R²=0.9983
R²=0.9989

Figure4b

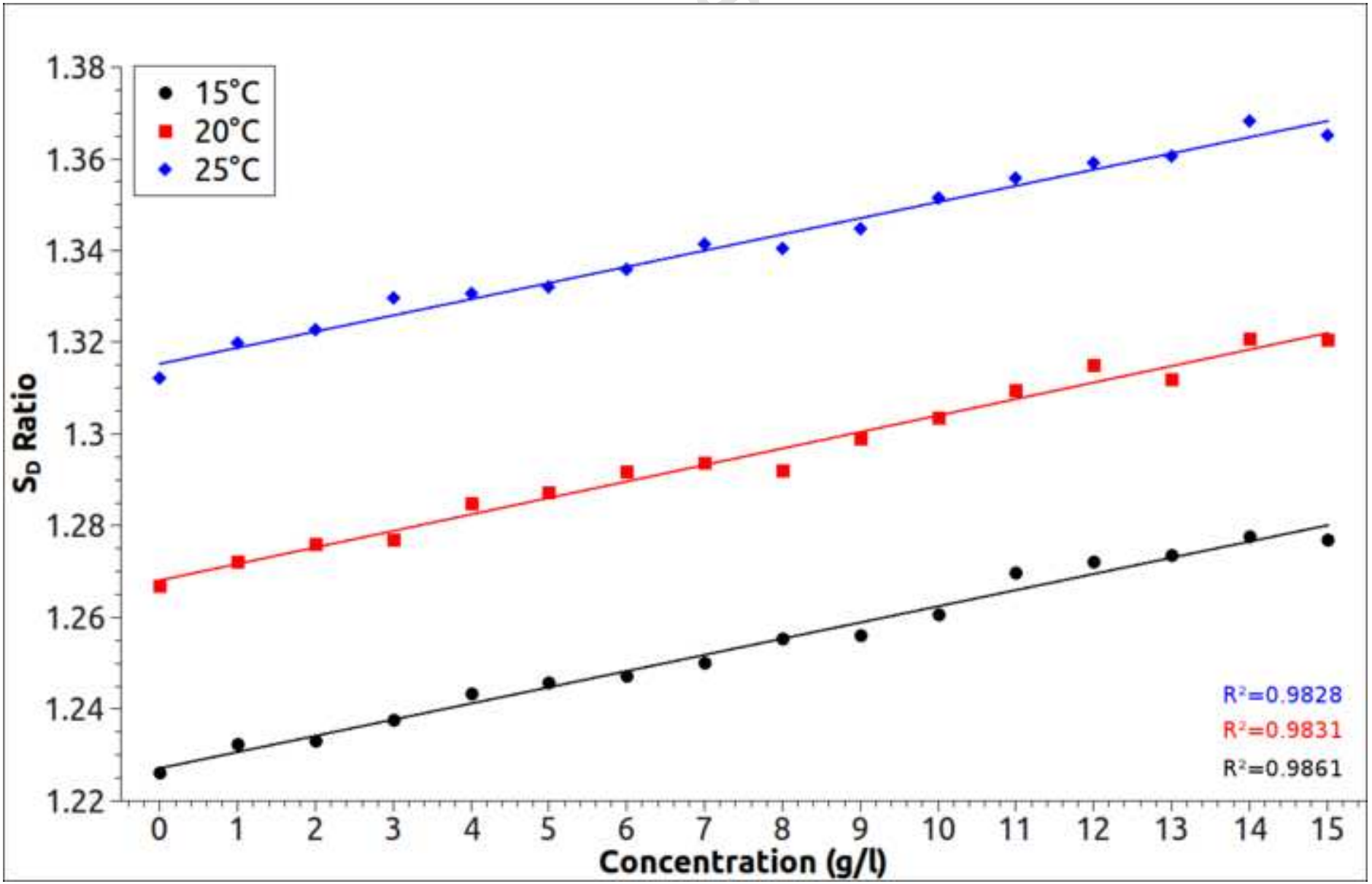
15°C
20°C
25°C
S_D Ratio
1.38
1.36
1.34
1.32
1.3
1.28
1.26
1.24
1.22
0
1
2
3
4
5
6
7
8
9
10
11
12
13
14
15
Concentration (g/l)
R²=0.9828
R²=0.9831
R²=0.9861

Figure5

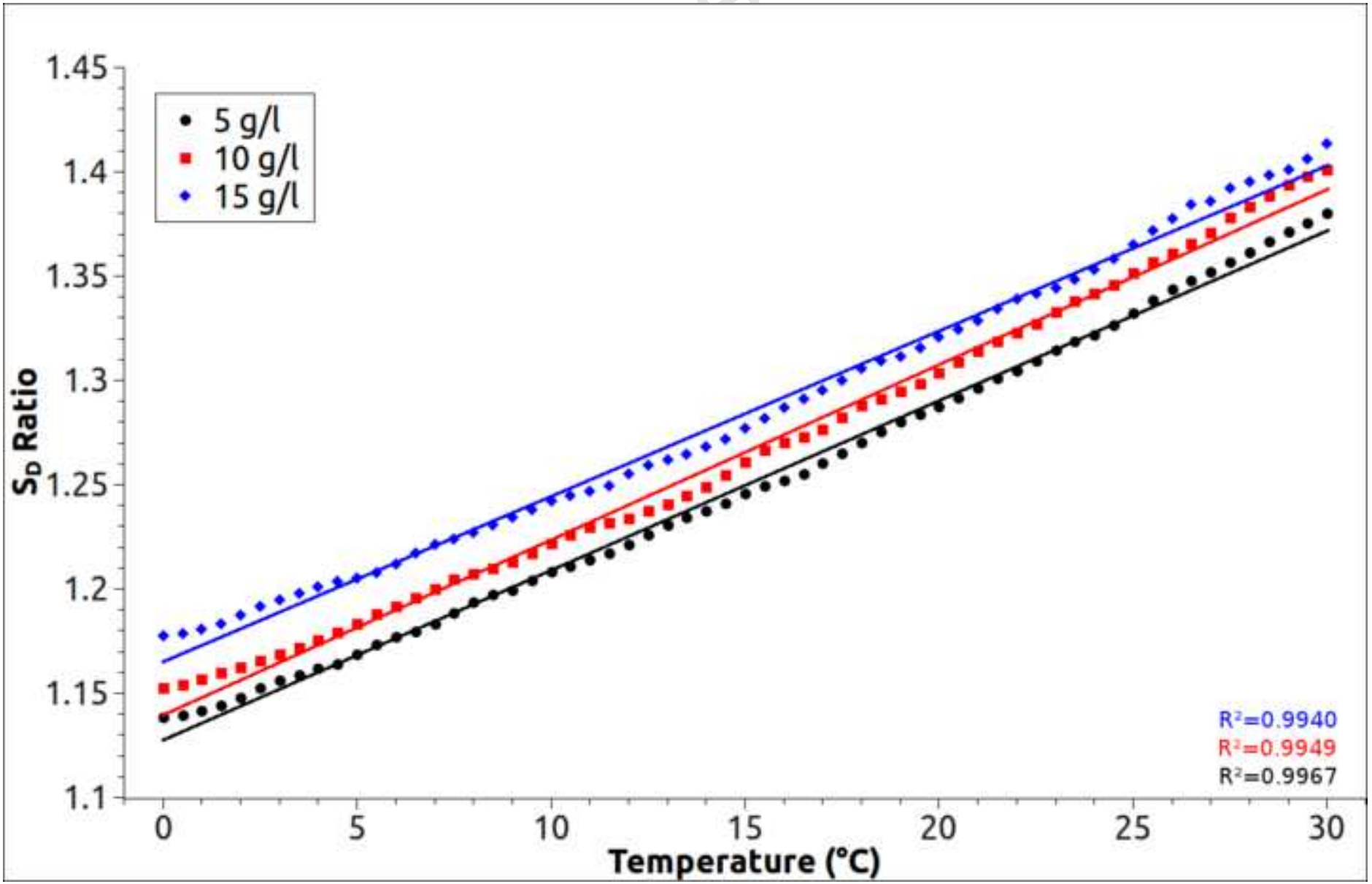
5 g/l
10 g/l
15 g/l
S_D Ratio
Temperature (°C)
1.45
1.4
1.35
1.3
1.25
1.2
1.15
1.1
0
5
10
15
20
25
30
R²=0.9940
R²=0.9949
R²=0.9967